HIGH-ORDER FINITE ELEMENT METHODS FOR SINGULARLY-PERTURBED ELLIPTIC AND PARABOLIC PROBLEMS*

SLIMANE ADJERID, MOHAMMED AIFFA, and

*JOSEPH E. FLAHERTY***

Dedicated to Joseph B. Keller on the Occasion of his Seventieth Birthday

Abstract. We develop a framework for applying high-order finite element methods to singularly-perturbed elliptic and parabolic differential systems that utilizes special quadrature rules to confine spurious effects, such as excess diffusion and non-physical oscillations, to boundary and interior layers. This approach is more suited for use with adaptive mesh-refinement and order-variation techniques than other problem-dependent methods. Quadrature rules, developed for two-point convection-diffusion and reaction-diffusion problems, are used with finite element software to solve examples involving ordinary and partial differential equations. Numerical artifacts are confined to layers for all combinations of meshes, orders, and singular perturbation parameters that were tested. Radau or Lobatto quadrature used with the finite element method to solve, respectively, convection- and reaction-diffusion problems provide the benefits of the specialized quadrature formulas and are simpler to implement.

Key words. adaptive finite element methods, Radau and Lobatto quadrature, high-order methods, singular perturbations

---

* This research was partially supported by the the U. S. Air Force Office of Scientific Research, Air Force Systems Command, USAF, under Grant Number AFOSR F49620-1-0218 and by the U. S. Army Research Office under Contract Number DAAL-03-91-G-0215.

** Scientific Computation Research Center, Rensselaer Polytechnic Institute, Troy, New York 12180. A portion of this research was done while the third author was on sabbatical leave at the Applied Mathematics and Mechanics Section, Benét Laboratories, Watervliet Arsenal, Watervliet, New York 12189.

AMS (MOS) subject classification. 65M20, 65M50, 65M60

1. Introduction. Beginning with a trial solution of a differential system computed on a coarse mesh with a low-order method, an adaptive strategy seeks to obtain a final solution satisfying prescribed discretization error criteria as quickly as possible. Tools for "enriching" the initial solution are denoted as h-, p-, or r-refinement when, respectively, the mesh is refined and coarsened, the order of the method is varied, or the mesh is moved to follow evolving phenomena. Enrichment, typically local in space, can be either local or global in time to produce, respectively, a local refinement method [1] or a method of lines [2]. The most successful adaptive enrichment techniques utilize a combination of the base strategies with the particular combination of hp-refinement capable of achieving exponential convergence rates [2-7].

Singularly-perturbed problems are ideal differential systems for adaptive analysis because it is far more efficient to resolve the nonuniform behavior within, e.g., boundary layers with nonuniform meshes and methods than with uniform structures. Current tools for adaptive analysis, however, lack a requisite robustness when applied to singularly-perturbed problems. Symmetric finite difference or finite element methods, commonly used with adaptive software, produce spurious oscillations (§2) when applied on a coarse mesh. Based on this incorrect solution, a correct error estimation could indicate global mesh refinement. While possibly successful, this strategy is far from optimal since refinement would most likely be necessary only within layers. "Upwinding" eliminates oscillations by adding diffusion, but successful strategies [8] are largely unknown for other than convection-diffusion systems. A posteriori error estimates, used to indicate adaptive enrichment, have been based on diffusive dominance for both elliptic and parabolic systems [9-11]; thus, minimally, their range of applicability is greatly diminished when they are applied to singularly-perturbed problems.

With a goal of developing high-order methods that may be used with adaptive hp-

refinement to solve singularly-perturbed partial differential systems, we develop a Galerkin finite element technique that utilizes special quadrature rules to attain stability (§2-4). Utilizing a hierarchical framework [12], the quadrature rules are designed to integrate products of exponential and polynomial functions to high order. In this regard, they bear some relationship to exponentially-weighted Petrov-Galerkin methods [13]; however, polynomials are used for both the finite element trial and test spaces. Thus, the new methods can be incorporated within an existing adaptive finite element system with only minor alterations. The singularly-perturbed limit of the derived quadrature rules for convection-diffusion systems are Radau integration formulas (§3). Radau (§3) and Lobatto (§4) quadrature yield stable computational results for, respectively, convection- and reaction-diffusion problems for all combinations of the singularly-perturbed parameter, the mesh spacing, and the order of the method. Large errors are confined to elements containing or adjacent to layers and may be reduced by either h- or p-refinement. Convergence rates remain optimal in the diffusion limit and, although rates are unknown, accuracy is high in the singularly-perturbed limit.

Quadrature rules are derived for ordinary differential systems and our methods may be useful with two-point boundary value problem software [14]. However, our intent is to use the derived rules with elliptic and parabolic partial differential systems through, e.g., tensor products and method of lines reduction. Thus, after verifying that the specialized, Radau, and Lobatto quadrature rules give good results when used with finite element procedures to solve ordinary convection-diffusion (§3) and reaction-diffusion (§4) systems, the methods are applied to one-dimensional transient (§3) and two-dimensional steady (§5) problems. Once again, the results display a robust behavior with large errors confined to regions of nonuniform behavior.

2. Formulation and Background. We illustrate the quadrature-based finite element method for the singularly-perturbed two-point boundary value problem

$$\mathbf{L}u := -\varepsilon u'' + c(x)u' + d(x)u = f(x), \quad a < x < b, \tag{2.1a}$$

$$u(a) = u_L, \quad u(b) = u_R, \tag{2.1b,c}$$

where $(\,)' := d(\,)/dx$. Assume that $\varepsilon > 0$ and consider cases when (i) $c(x) \neq 0$ or (ii) $c(x) := 0$ and $d(x) > 0$, $x \in [a,b]$. In the former case, convection dominates diffusion when the Reynolds or Peclet number $(b-a)\max_{a\le x\le b}|c(x)/\varepsilon|$ is large, and the solution of (2.1) has a boundary layer with thickness inversely proportional to the Peclet number at $x = a$ or b when c is, respectively, negative or positive. Reaction dominates diffusion in the latter case when $(b-a)[\max_{a\le x\le b} d(x)/\varepsilon]^{1/2}$ is large, and the solution of (2.1) features boundary layers near both a and b.

Consider the Galerkin form of (2.1): determine $u \in H^1_E$ satisfying

$$B(v,u) := \varepsilon(v',u') + (v,cu') + (v,du) = (v,f), \quad \text{for } all \ v \in H^1_0, \tag{2.2a}$$

where

$$(v,u) = \int_a^b v(x)u(x)\,dx, \tag{2.2b}$$

H^1 is the usual Sobolev space, and subscripts E or 0 restrict functions to, respectively, satisfy (2.1b,c) or trivial versions of (2.1b,c). A finite element problem is constructed from (2.2) by introducing a partition

$$\Pi_N := \{\, a = x_0 < x_1 < \cdots < x_N = b \,\} \tag{2.3}$$

of $[a\,,\,b]$ into N subintervals; defining a finite-dimensional space

$$S^{N,\mathbf{p}} = \{\, w \in H^1 \mid w(x) \in \Gamma_{p_i},\ x \in (x_{i-1},x_i),\ i = 1, 2, \cdots, N \,\}, \tag{2.4}$$

where $\mathbf{p} := [p_1, p_2, \cdots, p_N]^T$ and Γ_p is a space of polynomials of degree p; and determining $U \in S^{N,\mathbf{p}}_E$ satisfying

$$B(V,U) = (V,f), \quad \text{for } all \ V \in S^{N,\mathbf{p}}_0. \tag{2.5}$$

Representing $S^{N,\mathbf{p}}$ in terms of a hierarchical basis [12] is convenient, efficient, and

stable. Thus, we let

$$U(x) = \sum_{i=0}^{N} c_i \phi_i^1(x) + \sum_{i=1}^{N} \sum_{k=2}^{p_i} c_i^k \phi_i^k(x), \tag{2.6a}$$

where

$$\phi_i^1(x) = \begin{cases} \hat{\phi}_1(\xi(x)), & \text{if } x \in [x_{i-1}, x_i) \\ \hat{\phi}_{-1}(\xi(x)), & \text{if } x \in [x_i, x_{i+1}), \quad i = 0, 1, \cdots, N, \\ 0, & \text{otherwise} \end{cases} \tag{2.6b}$$

$$\phi_i^k(x) = \begin{cases} \hat{\phi}_k(\xi(x)), & \text{if } x \in [x_{i-1}, x_i) \\ 0, & \text{otherwise} \end{cases}, \quad k = 2, 3, \cdots, p_i, \quad i = 1, 2, \cdots, N, \tag{2.6c}$$

$$\xi(x) = \frac{2x - x_{i-1} - x_i}{x_i - x_{i-1}}, \tag{2.7a}$$

$$\hat{\phi}_{-1}(\xi) = (1 - \xi)/2, \quad \hat{\phi}_1(\xi) = (1 + \xi)/2, \tag{2.7b,c}$$

$$\hat{\phi}_k(\xi) = \sqrt{\frac{2k - 1}{2}} \int_{-1}^{\xi} P_{k-1}(\tau)\, d\tau = \frac{P_k(\xi) - P_{k-2}(\xi)}{\sqrt{2(2k - 1)}}, \quad \xi \in [-1,1], \tag{2.7d}$$

and $P_k(\xi)$ is the Legendre polynomial of degree k. The piecewise linear basis element $\phi_i^1(x)$ is associated with the node x_i while the higher-degree basis elements $\phi_i^k(x)$, $k = 2, 3, \cdots, p_i$, are associated with the subinterval (x_{i-1}, x_i). In order to simplify the subsequent presentation, let

$$\mathbf{\Phi} := \{ \phi_i^1(x),\ i = 0, 1, \cdots, N,\ \phi_i^k(x),\ k = 2, 3, \cdots, p_i,\ i = 1, 2, \cdots, N \}. \tag{2.8a}$$

With trivial Dirichlet boundary conditions, the dimension of $S_E^{N,\mathbf{p}}$ is

$$M = -1 + \sum_{i=1}^{N} p_i. \tag{2.8b}$$

Example 2.1. Some difficulties that arise when solving (2.1) by a conventional Galerkin-finite element approach can be illustrated for the simple example when c is a constant, $d(x) = f(x) := 0$, Π_N is uniform with spacing h, and $p_i = 1$, $i = 1, 2, \cdots, N$. In this case, the Galerkin coordinates satisfy

$$c_0 = u_L, \quad c_N = u_R, \tag{2.9a,b}$$

$$c_{i+1} - 2c_i + c_{i-1} = \frac{\rho}{2}(c_{i+1} - c_{i-1}), \quad i = 1, 2, \cdots, N-1, \tag{2.9c}$$

where $c_i = U(x_i)$, $i = 0, 1, \cdots, N$, and

$$\rho = \frac{ch}{\varepsilon} \tag{2.9d}$$

is the cell Peclet number. The solution of this difference equation is

$$c_i = \frac{\lambda^i - \lambda^N}{1 - \lambda^N} u_L + \frac{1 - \lambda^i}{1 - \lambda^N} u_R, \quad i = 0, 1, \cdots, N, \quad \lambda = \frac{2 + \rho}{2 - \rho}. \tag{2.9e,f}$$

The computationally challenging singularly-perturbed limit occurs when $\rho \gg 1$. In this case, c_i, $i = 0, 1, \cdots, N$, oscillates (i) between u_L and u_R when N is odd or (ii) between the line joining u_L and u_R and $2\rho/N$ when N is even. These spurious oscillations are only eliminated when the mesh is sufficiently fine, i.e., when ρ is reduced to $O(1)$ within the boundary layer.

The spurious oscillations can be eliminated from a convection-diffusion system by introducing a directional bias that adds artificial dissipation to the system. Although schemes for accomplishing this abound for convection-diffusion systems (cf., e.g., Il'in [15]), Hemker's [13] Petrov-Galerkin formulation has a generality that best suits our present aims. To begin, recall that the Green's function $G(t,x)$ for the operator $\mathbf{L}$ of (2.1) is an element of H_0^1 for fixed t that satisfies

$$\mathbf{L}^*G = -\varepsilon G_{xx} - [c(x)G]_x + d(x)G = 0, \quad a < x < t, \; t < x < b, \tag{2.10a}$$

$$[G_x(t,t)]_{x=t} := \lim_{\delta \to 0} [G_x(t,t+\delta) - G_x(t,t-\delta)] = -\frac{1}{\varepsilon}, \tag{2.10b}$$

where an x subscript denotes partial differentiation. With this definition, we readily show [13] that

$$v(t) = B(G(t,\cdot),v), \quad \text{for } all \; v \in H^1. \tag{2.11}$$

Consider the Petrov-Galerkin problem: determine $U \in S_E^{N,\mathbf{p}}$ satisfying

$$B(\tilde{V},U) = (\tilde{V},f), \quad \text{for all } \tilde{V} \in \tilde{S}_0^{N,\mathbf{p}}. \tag{2.12}$$

Like $S_0^{N,\mathbf{p}}$, the space $\tilde{S}_0^{N,\mathbf{p}}$ is a finite-dimensional subspace of H_0^1; however, it consists of piecewise polynomial and exponential functions. We'll identify a basis for $\tilde{S}_0^{N,\mathbf{p}}$ as

$$\Psi := \{ \psi_i^1(x),\ i = 0, 1, \cdots, N,\ \psi_i^k(x),\ k = 2, 3, \cdots, p_i,\ i = 1, 2, \cdots, N \}, \tag{2.13}$$

but defer more specific definitions of its components until (2.16), §3, and §4.

Replacing v by $\tilde{V}$ in (2.2a) and subtracting (2.12) from the result yields the orthogonality relationship

$$B(\tilde{V},e) := B(\tilde{V},u-U) = 0, \quad \text{for all } \tilde{V} \in \tilde{S}_0^{N,\mathbf{p}}. \tag{2.14}$$

Replacing v by e in (2.11) and subtracting (2.14) from the result yields

$$e(t) = B(G(t,\cdot) - \tilde{V},e), \quad \text{for all } \tilde{V} \in \tilde{S}_0^{N,\mathbf{p}}. \tag{2.15a}$$

With $B(v,u)$ continuous, we confine t to Π_N and obtain

$$|e(x_i)| \le C\|G(x_i,\cdot) - \tilde{V}\|_1 \|e\|_1, \quad \text{for all } \tilde{V} \in \tilde{S}_0^{N,\mathbf{p}}, \quad i = 0, 1, \cdots, N. \tag{2.15b}$$

The estimate (2.15b) indicates that the pointwise error of the Petrov-Galerkin scheme (2.12) can be reduced by making $\|e\|_1$ and/or $\|G(x_i,\cdot) - \tilde{V}\|_1$ small. Satisfying one option usually leads to the other; however, trial and test functions can differ significantly for singularly-perturbed problems. Using (2.15), Hemker [13] argued that $\tilde{S}_0^{N,\mathbf{p}}$ should be selected to produce good approximations of $G(x_i,x)$. This usually implies that $\tilde{S}_0^{N,\mathbf{p}}$ should accurately represent the rapidly varying exponential portion of $G(x_i,x)$ that occurs at $x = x_i$ and a and/or b [16].

Example 2.2. Consider the Petrov-Galerkin solution of (2.1) under the conditions of Example 2.1. Using piecewise linear approximations for $S_E^{N,1}$, choose a basis for $\tilde{S}_0^{N,1}$ that exactly satisfies (2.10) when c is a constant, $d := 0$, and $t \in \Pi_N$, i.e., choose

$$\psi_i^1(x) = \begin{cases} \hat{\psi}_1(\xi(x)), & \text{if } x \in [x_{i-1},x_i) \\ \hat{\psi}_{-1}(\xi(x)), & \text{if } x \in [x_i,x_{i+1}), \quad i = 0, 1, \cdots, N, \\ 0, & \text{otherwise} \end{cases} \tag{2.16a}$$

where

$$\hat{\psi}_{-1}(\xi) = 1 - \hat{\psi}_1(\xi), \quad \hat{\psi}_1(\xi) = \frac{1 - e^{-\rho(1+\xi)/2}}{1 - e^{-\rho}}. \tag{2.16b,c}$$

The shape functions (2.16b,c) reduce to the linear functions (2.7c,d) as $\rho \to 0$ and have jump discontinuities at $\xi = -1$ as $\rho \to \infty$ (cf. Fig. 1).

Using (2.6, 7) and (2.16) in (2.12) leads to the discrete system

$$[1 + \frac{\rho}{2}\omega(\frac{\rho}{2})](c_{i+1} - 2c_i + c_{i-1}) = \frac{\rho}{2}(c_{i+1} - c_{i-1}), \quad i = 1, 2, \cdots, N - 1, \tag{2.17a}$$

with

$$\omega(z) = \coth z - \frac{1}{z} \tag{2.17b}$$

and the boundary conditions (2.9a,b). This scheme, which is identical to Il'in's [15] finite difference scheme, yields a pointwise-exact solution of (2.1) under the conditions of this example.

A Petrov-Galerkin scheme such as (2.12) would require a major re-coding effort to incorporate into a state-of-the-art adaptive finite element software system (cf., e.g., Adjerid et al. [2]). This effort would, furthermore, have to be duplicated for different singular perturbations. Finite element schemes typically use numerical quadrature to evaluate inner products; thus, instead of solving (2.5), a solution $W^* \in S_E^{N,\mathbf{p}}$ is determined from

$$B_*(V, W^*) = (V, f)_*, \quad \text{for } \textit{all } V \in S_0^{N,\mathbf{p}}, \tag{2.18}$$

where the * indicates that integrals are evaluated using a quadrature rule.

Example 2.3. Hughes [17] recognized that the diffusion needed to stabilize the piecewise-linear Galerkin solution of convection-diffusion problems could be added by a one-point quadrature rule of the form

$$\int_{-1}^{1} f(\xi)\, d\xi \approx 2f(\xi_1), \quad \xi_1 = \omega(\frac{\rho}{2}). \tag{2.19}$$

This, when used with (2.18), yields the Petrov-Galerkin discrete system (2.17). The quadrature rule (2.19) depends on ρ and approaches the midpoint rule ($\xi_1 = 0$) in the diffusion limit $\rho \to 0$ and the Radau formula ($\xi_1 = \text{sgn}\rho$) in the convection limit $\rho \to \infty$.

Hughes's [17] approach only requires a change of quadrature rule and is, thus, simpler to implement than a Petrov-Galerkin method. Piecewise-polynomial bases (2.8a) are used for both trial and test spaces and the technique may be extended to higher-order approximations and other than convection-diffusion problems. Thus, we seek to develop a framework for the design of quadrature rules that are appropriate for the finite-element Galerkin solution of singularly-perturbed problems.

3. Quadrature-Based Scheme for Convection-Diffusion Problems. Quadrature rules for convection-dominated problems are developed for problems having the form of (2.1) with $c(x) \neq 0$ and $d(x) := 0$, $x \in [a,b]$. We begin by defining a mapping between the polynomial and exponential spaces and use this to obtain a result similar to (2.15) which motivates the approach.

DEFINITION 3.1. Let $V(x) \in S_0^{N,\mathbf{p}}$ be given by (2.6a), with $c_0 = c_N = 0$ and let $F: S_0^{N,\mathbf{p}} \to \tilde{S}_0^{N,\mathbf{p}}$ be the mapping

$$V \to F(V) = \tilde{V} = \sum_{i=1}^{N-1} c_i \psi_i^1(x) + \sum_{i=1}^{N} \sum_{k=2}^{p_i} c_i^k \psi_i^k(x). \tag{3.1}$$

LEMMA 3.1. *Let*

$$U^*(x) = \sum_{i=0}^{N} c_i^* \phi_i^1(x) + \sum_{i=1}^{N} \sum_{k=2}^{p_i} c_i^{*,k} \phi_i^k(x) \tag{3.2a}$$

be an element of $S_E^{N,\mathbf{p}}$ *that satisfies (2.18), then*

$$e^*(x_i) := u(x_i) - U^*(x_i) = B(G(x_i,\cdot) - F(V), e^*) + B_*(V,U^*) - B(F(V),U^*) +$$

$$(F(V),f) - (V,f)_*, \quad \text{for } all \ V \in S_0^{N,\mathbf{p}}, \quad i = 0, 1, \cdots, N. \tag{3.2b}$$

Proof. Replacing v by e^* in (2.11), adding and subtracting $B(F(V),e^*)$ to the right

side of the result, and using (2.18) gives (3.2b). □

Using (3.2b), we see that the pointwise error can be reduced by (i) selecting Ψ to be a good approximation of the Green's function in order to minimize $\|B(G(x_i,\cdot) - \tilde{V}\|$ and (ii) designing a quadrature rule to minimize $\|B_*(V,W^*) - B(F(V),U^*)\|$ and $\|(F(V),f) - (V,f)_*\|$, for *all* $V \in S_0^{N,\mathbf{p}}$. As a compromise, we'll select $\tilde{V}$ and develop quadrature rules so that $\|B_*(V,W^*) - B(F(V),U^*)\|$ vanishes for locally constant-coefficient problems. Thus, using (2.6c) to transform integrals on (x_{i-1},x_i) to $(-1,1)$, we require

$$\hat{B}_*(\hat{\phi}_k,\xi^l) = \hat{B}(\hat{\psi}_k,\xi^l), \quad k = -1, 1, 2, \cdots, p, \quad l = 0, 1, \cdots, p, \tag{3.3a}$$

where

$$\hat{B}(v,u) = \int_{-1}^{1} [v'(\xi)u'(\xi) + \frac{\rho}{2}v(\xi)u'(\xi)]\, d\xi \tag{3.3b}$$

and the quadrature rule has the form

$$\left[\int_{-1}^{1} f(\xi)\, d\xi\right]_* = \sum_{k=1}^{n} W_k f(\xi_k). \tag{3.4}$$

Elemental indices i on the cell Peclet number ρ and the polynomial degree p have been omitted for convenience.

Setting $p = 1$ and using (3.3) with $\hat{\psi}_{\pm 1}(\xi)$ given by (2.16b,c) and $\hat{\phi}_{\pm 1}(\xi)$ given by (2.7b,c) leads to Hughes' [17] one-point quadrature rule (2.19). Analysis of another example with $p = 2$ will further illustrate the technique without the algebraic complexity of the more general case to be developed subsequently.

Example 3.1 (Two-Point Quadrature Rule). Bases for the trial and test spaces for a two-point ($n = 2$) quadrature rule are selected as

$$\hat{\mathbf{\Phi}} = \{\hat{\phi}_{-1}, \hat{\phi}_1, \hat{\phi}_2\}, \quad \hat{\mathbf{\Psi}} = \{\hat{\phi}_{-1}, \hat{\phi}_1, \hat{\psi}_2\}, \tag{3.5a,b}$$

where

$$\hat{\psi}_2(\xi) = \frac{\hat{\psi}_1(\xi) - \hat{\phi}_1(\xi)}{\alpha_2} \tag{3.5c}$$

and the scaling factor α_2 must be determined (cf. Fig. 1). The bases (3.5a) and (3.5b) agree except for the last component which contains the exponential contribution to the Green's function. The shape functions $\hat{\phi}_2$ is shown in Fig. 1. As $\rho \to 0$, $\hat{\psi}_2(\xi)$ tends to the polynomial shape function $\hat{\phi}_2(\xi)$ and as $\rho \to \infty$, $\hat{\psi}_2(\xi)$ becomes linear outside of an $O(1/\rho)$ boundary layer at $\xi = -1$.

Setting $p = 2$ in (3.3) and using (3.5) yields the conditions

$$W_1\xi_1^k + W_2\xi_2^k = \int_{-1}^{1} \xi^k \, d\xi, \quad k = 0, 1, 2, \tag{3.6a}$$

$$\hat{B}_*(\hat{\phi}_2,\xi^l) = \hat{B}(\hat{\psi}_2,\xi^l), \quad l = 1, 2. \tag{3.6b}$$

This nonlinear system is readily solved to obtain

$$\xi_{1,2} = \frac{3m_3}{4} \pm \sqrt{(\frac{3m_3}{4})^2 + \frac{1}{3}}, \quad W_1 = \frac{2\xi_2}{\xi_2 - \xi_1}, \quad W_2 = -\frac{2\xi_1}{\xi_2 - \xi_1}, \tag{3.7a-d}$$

where

$$\alpha_2 = -\sqrt{\frac{3}{2}}\omega(\frac{\rho}{2}), \quad m_3 = \frac{4}{9}(\frac{1}{\omega(\rho/2)} - \frac{6}{\rho}), \tag{3.7e,f}$$

and $\omega(z)$ was defined by (2.17b). As $\rho \to 0$, (3.7) becomes Gauss-Legendre quadrature ($\xi_{1,2} = \pm 1/\sqrt{3}$, $W_1 = W_2 = 1$) and as $\rho \to \infty$, (3.7) becomes Radau quadrature ($\xi_1 = -1/3$, $\xi_2 = 1$, $W_1 = 3/2$, $W_2 = 1/2$).

We proceed in the same manner with a general (n-point) quadrature rule, selecting

$$\hat{\mathbf{\Phi}} = \{ \hat{\phi}_{-1}, \hat{\phi}_1, \hat{\phi}_2, \cdots, \hat{\phi}_n \}, \quad \hat{\mathbf{\Psi}} = \{ \hat{\phi}_{-1}, \hat{\phi}_1, \hat{\phi}_2, \ldots, \hat{\phi}_{n-1}, \hat{\psi}_n \}, \tag{3.8a,b}$$

where

$$\hat{\psi}_n(\xi) = \frac{\hat{\psi}_{n-1}(\xi) - \hat{\phi}_{n-1}(\xi)}{\alpha_n}, \quad n \geq 2. \tag{3.8c}$$

The shape functions $\hat{\psi}_3(\xi)$ and $\hat{\psi}_4(\xi)$ are shown in Fig. 1.

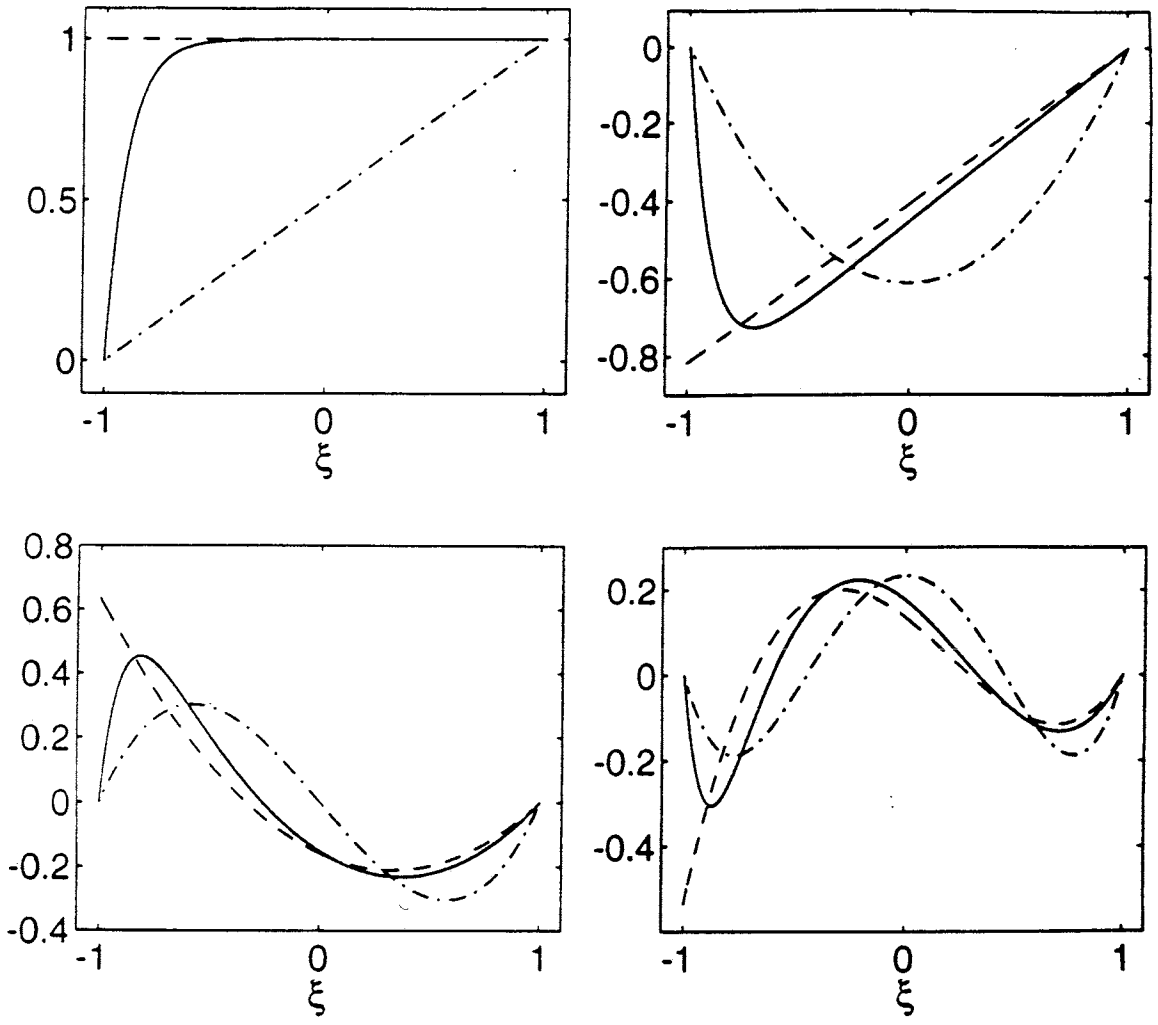

FIG. 1. Shape functions $\hat{\psi}_p(\xi)$, $p = 1, 2, 3, 4$ (upper left, upper right, lower left, lower right), for $\rho = 0, 10, \infty$ (dash-dot, solid, dash). Functions with $\rho = 0$ correspond to $\hat{\phi}_p(\xi)$, $p = 1, 2, 3, 4$.

The use of (3.8) with (3.3, 4) yields the system

$$\sum_{l=1}^{n} W_l \xi_l^k = \int_{-1}^{1} \xi^k \, d\xi, \quad k = 0, 1, \cdots, 2n - 2, \tag{3.9a}$$

$$\hat{B}_*(\hat{\phi}_n, \xi^l) = \hat{B}(\hat{\psi}_n, \xi^l), \quad l = n - 1, n, \tag{3.9b}$$

which may be written in the more explicit form

$$\alpha_n = \frac{1}{\int_{-1}^{1} \hat{\phi}_n(\xi)\xi^{n-2} d\xi} \begin{cases} \int_{-1}^{1} [\hat{\psi}_1(\xi) - \hat{\phi}_1(\xi)] d\xi, & \text{if } n = 2 \\ \int_{-1}^{1} \hat{\psi}_{n-1}(\xi)\xi^{n-2} d\xi, & \text{if } n > 2 \end{cases}, \tag{3.10a}$$

$$\sum_{l=1}^{n} W_l \xi_l^{2n-1} = m_{2n-1} = \frac{n!}{\hat{\phi}_n^{(n)}(0)} \int_{-1}^{1} \hat{\psi}_n(\xi)\xi^{n-1} d\xi. \tag{3.10b}$$

The nonlinear system (3.9a, 10) may be solved for $n \leq 4$ using a computer algebra system such as *MAPLE*. With $n = 3$, for example, the integration points ξ_l, $l = 1, 2, 3$, are determined as the roots of

$$\xi^3 - \frac{45m_5}{8}\xi^2 - \frac{3}{5}\xi + \frac{15m_5}{8} = 0, \tag{3.11a}$$

with

$$m_5 = \frac{32}{675}\left(\frac{1}{m_3} - \frac{45}{2\rho}\right), \quad \alpha_3 = -\frac{3m_3\sqrt{15}}{4}. \tag{3.11b,c}$$

When $n = 4$, the integration points are the roots of

$$\xi^4 - \frac{175m_7}{8}\xi^3 - \frac{6}{7}\xi^2 + \frac{105m_7}{8}\xi + \frac{3}{35} = 0, \tag{3.12a}$$

with

$$m_7 = \frac{32}{175}\left(\frac{8}{525m_5} - \frac{2}{\rho}\right), \quad \alpha_4 = -\frac{15m_5\sqrt{35}}{8}. \tag{3.12b,c}$$

While the quadrature weights W_l and evaluation points ξ_l, $l = 1, 2, \cdots, n$, cannot be explicitly determined as functions of ρ for $n > 4$, apparently they tend to the Gauss-

Legendre weights and points as $\rho \to 0$ and to the Radau weights and points as $\rho \to \infty$. This situation is favorable to adaptive h-refinement since (as we shall show by example) the quadrature-based finite element method is very stable in the convective limit and accurate in the diffusion limit.

3.1. Computational Results. We appraise the quadrature-based finite element method (2.18) by applying it to problems involving one ordinary and two partial differential systems. In each case, the Green's function used to develop the quadrature rule (3.4) is inaccurate; hence, we hope to show that $\hat{\Psi}$ only has to capture the essence of the singular portion of the adjoint space to obtain the desired stability. We also show that Radau quadrature provides essentially the same benefits as more complex quadrature rules depending on the cell Peclet number. As in the derivation, the local degree of the polynomial approximation p is the same as the number of points n used for the quadrature rule.

In each example, pointwise errors are measured in the discrete maximum norm

$$|e^*|_\infty = \max_{x \in \Pi_{N_1}} |e^*(x)| \tag{3.13}$$

where N_1 is the number of elements in the coarsest mesh used to solve the problem. Spatial complexity is measured by the degrees of freedom which, with Dirichlet boundary data, is M according to (2.8b).

Example 3.2. Consider the two-point problem [13]

$$-\varepsilon u'' - xu' = \varepsilon\pi^2\cos(\pi x) + \pi x \sin(\pi x), \quad -1 < x < 1, \tag{3.14a}$$

$$u(-1) = -2, \quad u(1) = 0, \tag{3.14b,c}$$

which has the exact solution

$$u(x) = \cos(\pi x) + \frac{\operatorname{erf}(x/\sqrt{2\varepsilon})}{\operatorname{erf}(1/\sqrt{2\varepsilon})}. \tag{3.14d}$$

The solution (3.14d) is smooth outside of a shock layer in the turning-point region near $x = 0$.

We solved (3.14) on uniform meshes having 20, 40, and 80 elements with piecewise polynomials of uniform degrees p = 1, 2, 3, 4 and values of $\varepsilon = 10^{-2}$, 10^{-6}, and 10^{-10}. Maximum errors on the (N_1 =) 20-element mesh using the finite element method with the ρ-dependent quadrature rules derived from (3.4, 8-10) and with Radau quadrature rules are presented in Table 1 as functions of p, N, and ε. In Fig. 2, we display $|e^*|_\infty$ with $\varepsilon = 10^{-6}$ as a function of the degrees of freedom for p ranging from 1 to 4 using (3.4, 8-10) and Radau quadrature. Similarly, with N = 80, we display $|e^*|_\infty$ as a function of ε for p = 1 to 4 in Fig. 3. Finally, the finite element solution using Radau quadrature is compared with the exact solution when $\varepsilon = 10^{-6}$, N = 20, and p = 1 to 4 in Fig. 4.

TABLE 1

Maximum errors $|e^*|_\infty$ for Example 3.2 using integration formula (3.4, 8-10) and Radau quadrature on uniform N-element meshes with piecewise polynomials of uniform degree p.

p	N	Eqs. (3.4, 8-10)		Radau	
		$\varepsilon = 10^{-2}$	$\varepsilon = 10^{-10}$	$\varepsilon = 10^{-2}$	$\varepsilon = 10^{-10}$
1	20	0.109(0)	0.149(0)	0.182(0)	0.148(0)
	40	0.402(-1)	0.765(-1)	0.981(-1)	0.764(-1)
	80	0.119(-1)	0.388(-1)	0.519(-1)	0.387(-1)
	20	0.124(-2)	0.142(-3)	0.526(-2)	0.142(-3)
	40	0.843(-4)	0.179(-4)	0.734(-3)	0.178(-4)
	80	0.533(-5)	0.224(-5)	0.988(-4)	0.223(-5)
3	20	0.318(-4)	0.769(-5)	0.167(-3)	0.107(-4)
	40	0.659(-6)	0.483(-6)	0.560(-5)	0.675(-6)
	80	0.118(-7)	0.302(-7)	0.188(-6)	0.422(-7)
4	20	0.538(-6)	0.400(-7)	0.444(-5)	0.400(-7)
	40	0.223(-8)	0.136(-9)	0.341(-7)	0.942(-11)
	80	0.875(-11)	0.302(-11)	0.272(-9)	0.186(-10)

Finite element solutions on Π_{N_1} displayed in Table 1 and Figs. 2 and 3 have no spurious oscillations for all cell Peclet numbers. Nodal convergence improves as p increases; however, there is an $O(\varepsilon)$ error that cannot be removed without proper resolution of the solution within the turning-point region. (This phenomena also occurs with boundary layer problems.) The special quadrature rules (3.4, 8-10) produce solutions that are slightly better than those obtained with Radau quadrature, but the difference may not

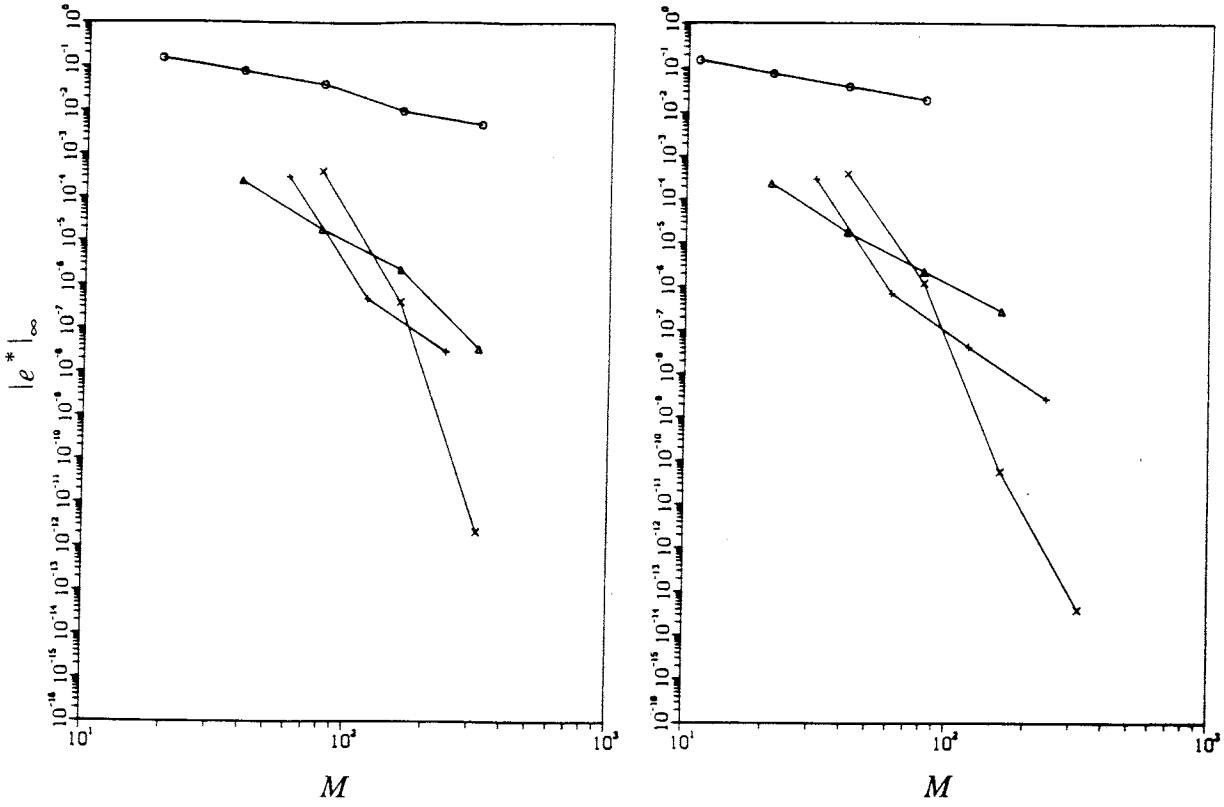

FIG. 2. Maximum errors $|e^*|_\infty$ vs. degrees of freedom M for Example 3.2 using integration formula (3.4, 8-10) (left) and Radau quadrature (right). Uniform mesh and order computations correspond to $p = 1$ (○), 2 (Δ), 3 (+), and 4 (×).

be worth the added expense. Results presented in Fig. 4 show that the finite element-Radau solution has some excess diffusion when $p = 1$ and some spurious oscillations when $p > 1$; however, these undesirable effects are confined to the two elements containing the turning point. The oscillations decrease in magnitude as p increases and the polynomial basis provides a better approximation to the exponential boundary layer behavior. Approximations would likewise improve were the mesh refined in the turning-point region. Global accuracy away from the turning point is very high.

Example 3.3. In order to appraise the method's suitability for use with transient problems, consider Burgers' equation

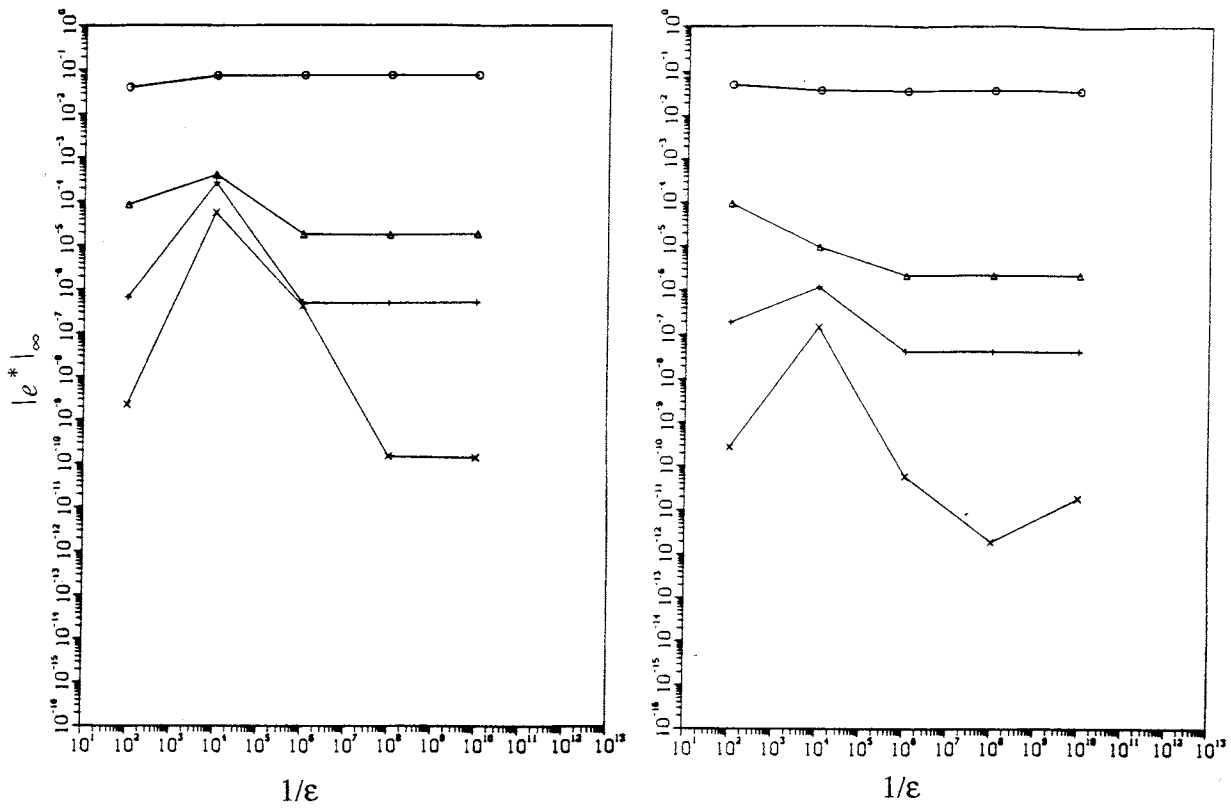

FIG. 3. Maximum errors $|e^*|_\infty$ vs. $1/\varepsilon$ for Example 3.2 using integration formula (3.4, 8-10) (left) and Radau quadrature (right). Uniform mesh computations with $N = 80$ were performed with uniform degrees of $p = 1$ (○), 2 (Δ), 3 (+) and 4 (×).

$$u_t + uu_x = \varepsilon u_{xx}, \quad 0 < x < 1, \quad t > 0, \tag{3.15a}$$

with initial and Dirichlet boundary conditions prescribed so that the exact solution is the traveling wave [18]

$$u(x,t) = \frac{0.1e^{-A} + 0.5e^{-B} + e^{-C}}{e^{-A} + e^{-B} + e^{-C}} \tag{3.15b}$$

with $\varepsilon = 3\times 10^{-3}$ and

$$A = \frac{0.05}{\varepsilon}(x - 0.5 + 4.95t), \quad B = \frac{0.25}{\varepsilon}(x - 0.5 + 0.75t), \quad C = \frac{0.5}{\varepsilon}(x - 0.375). \tag{3.15c-e}$$

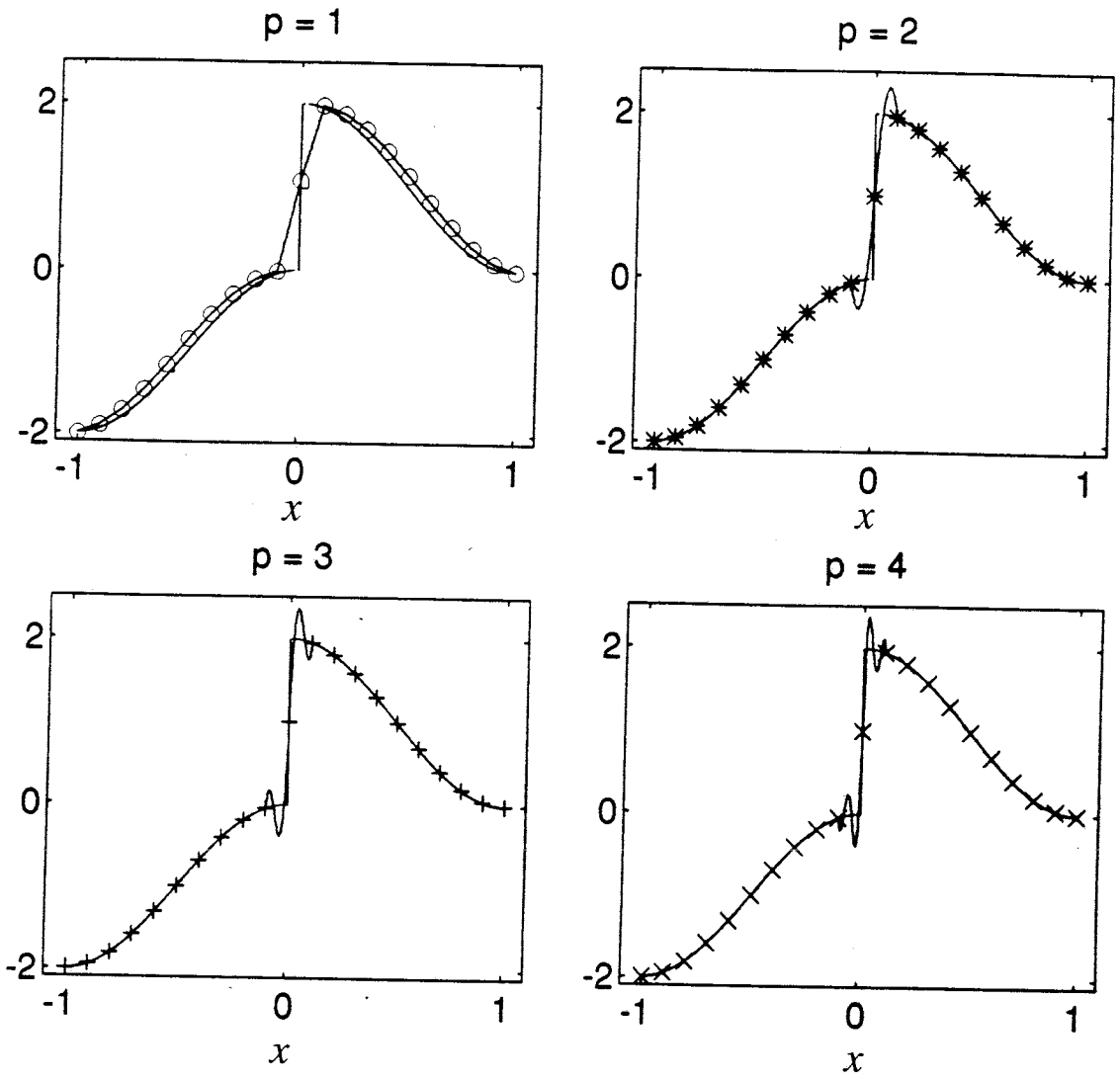

FIG. 4. Finite element solution using Radau quadrature and exact solution of Example 3.2 with $\varepsilon = 10^{-6}$, $N = 20$ and $p = 1$ (○), 2 (*), 3 (+) and 4 (×).

The cell Peclet number, needed for use with (3.4, 8-10), was determined from (2.9d) with c replaced by the average of the convective velocity U^* at both ends of an element. We solved (3.15) for $0 < t \leq 0.5$ on a uniform 80-element mesh using piecewise polynomials having uniform degrees of one to four. Temporal integration used the backward difference code *DASSL* [19] with an error tolerance of 10^{-10}. The exact solution and the

finite element solution using (3.4, 8-10) are compared as functions of x at $t = 0.5$ in Fig. 5 for $p = 1, 2$. Results with $p = 3$ and 4 could not be distinguished from the exact solution. The piecewise linear solution shown on the left of Fig. 5 has too much dissipation and an incorrect wave speed. The piecewise quadratic solution has remedied these deficiencies.

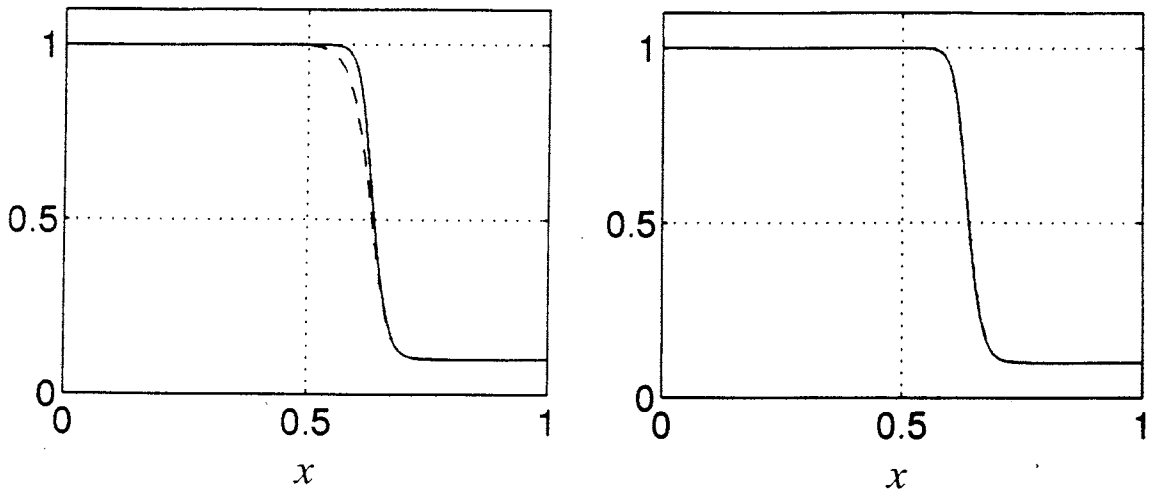

FIG. 5. Finite element (dashed) and exact (solid) solutions of Example 3.3 at $t = 0.5$ using a uniform 80-element mesh and piecewise polynomials of uniform degree one (left) and two (right).

Example 3.4. Consider the nonlinear initial-boundary value problem [20]

$$\varepsilon u_t + u(u^2-1)u_x + u = \varepsilon u_{xx}, \quad 0 < x < 1, \quad t > 0, \tag{3.16a}$$

$$u(x,0) = (x + 3)/2, \quad 0 \le x \le 1, \tag{3.16b}$$

$$u(0,t) = 3/2, \quad u(1,t) = 2, \quad t > 0. \tag{3.16c,d}$$

The solution of (3.16) tends to a steady state as $t \to \infty$ and time has been scaled to quickly reach this limit. An analysis when $0 < \varepsilon \ll 1$ [20] reveals that the steady solution features an interior layer near $x = 0.096$, a corner layer near $x = 0.333$, and a boundary

layer at $x = 1$.

Equations (3.16) were solved for $t \in (0,0.1]$ with $\varepsilon = 10^{-3}$ using adaptive h-refinement with uniform piecewise quadratic polynomials [2], an H^1 spatial error tolerance of 0.1, and a temporal error tolerance of 10^{-4}. The finite element solution, computed with (3.4, 8-10) using cell Peclet numbers as specified in Example 3.3, and the mesh constructed by the adaptive procedure are shown in Fig. 6. The solution differed from one computed using Gauss-Legendre quadrature by less than 2×10^{-3} in strain energy; however, the solution obtained using (3.4, 8-10) used 20% fewer space-time degrees of freedom. The adaptive mesh is concentrated in layers and little element removal was necessary. Meshes track evolving layers from the smooth initial data. The solution obtained with Gauss-Legendre quadrature performed well here because h-refinement occurred quickly as layers developed.

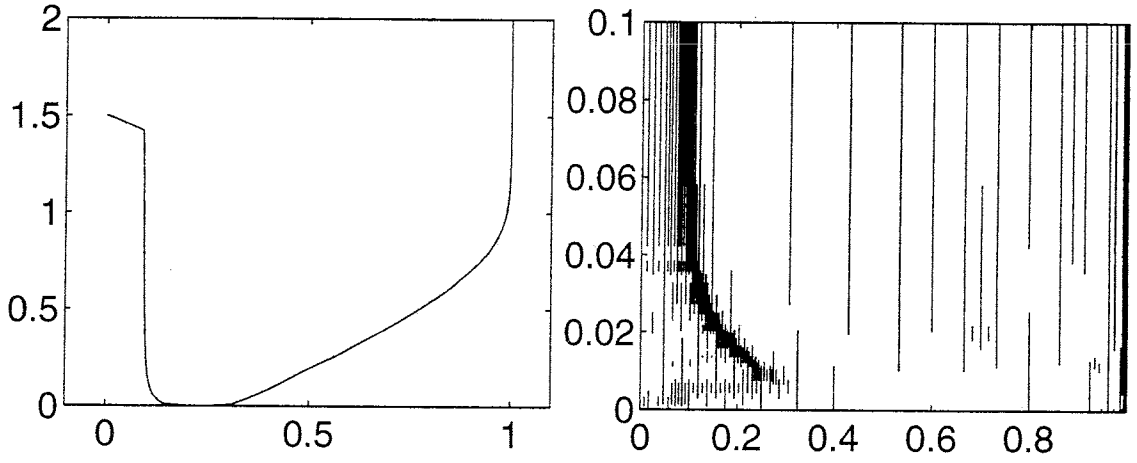

FIG. 6. Finite element solution of Example 3.4 at $t = 0.2$ using the quadrature rules (3.4, 8-10) with adaptive h-refinement and $p = 2$ (left) and the mesh used for the adaptive computation (right).

4. Quadrature-Based Scheme for Reaction-Diffusion Problems. We develop quadrature rules for reaction-diffusion problems of the form of (2.1) with $c(x) := 0$ and $d(x) > 0$ using the approach described in §3. The analog of Lemma 3.1 has a slightly more complex form.

LEMMA 4.1. *Let* $\mathbf{\Phi}$ *of (2.8a) and*

$$\mathbf{H} := \{ \eta_i^1(x),\ i = 0, 1, \cdots, N,\ \eta_i^k(x),\ k = 2, 3, \cdots, p_i,\ i = 1, 2, \cdots, N \}, \tag{4.1}$$

be two bases of $S_E^{N,\mathbf{p}}$. *Let*

$$W^*(x) = \sum_{i=0}^{N} c_i^* \phi_i^1(x) + \sum_{i=1}^{N} \sum_{k=2}^{p_i} c_i^{*,k} \phi_i^k(x) \tag{4.2a}$$

satisfy (2.18) and

$$U^*(x) = \sum_{i=0}^{N} c_i^* \eta_i^1(x) + \sum_{i=1}^{N} \sum_{k=2}^{p_i} c_i^{*,k} \eta_i^k(x). \tag{4.2b}$$

Then

$$e^*(x_i) := u(x_i) - U^*(x_i) = B(G(x_i,\cdot) - F(V), e^*) + B_*(V, W^*) - B(F(V), U^*)$$

$$(F(V), f) - (V, f)_*, \quad \text{for all } V \in S_0^{N,\mathbf{p}}, \quad i = 0, 1, \cdots, N. \tag{4.3}$$

Remark. The elements of $\mathbf{H}$ will be chosen to be identical to those of $\mathbf{\Phi}$ except for $\eta_i^{p_i}$ which will differ from $\phi_i^{p_i}$, $p_i > 1$, by a scaling factor, $i = 1, 2, \cdots, N$. The scaling is necessary to avoid a constant difference between exact and numerical inner products.

Proof. A direct computation following the steps of Lemma 1 yields the result. □

As a function of x, the Green's function in this case has $O(\sqrt{\varepsilon})$ boundary layers on both sides of $x = t$ and becomes unbounded as $O(1/\sqrt{\varepsilon})$ as $\varepsilon \to 0$ [16]. Requiring $\|B_*(V, W^*) - B(F(V), U^*)\|$ to vanish for locally constant-coefficient problems and transforming via (2.7a) to the canonical element $(-1,1)$, we obtain

$$\hat{B}_*(\hat{\phi}_k, \hat{\phi}_l) = \hat{B}(\hat{\psi}_k, \hat{\eta}_l), \quad k, l = -1, 1, 2, \cdots, p, \tag{4.4a}$$

where now

$$\hat{B}(v,u) = \int_{-1}^{1} [v'(\xi)u'(\xi) + \frac{\sigma^2}{4} v(\xi)u(\xi)]\, d\xi, \quad \sigma = h\sqrt{\frac{d}{\varepsilon}}. \tag{4.4b,c}$$

For this self-adjoint problem, we select a symmetric quadrature rule of the form

$$\left[\int_{-1}^{1} f(\xi)\, d\xi\right]_* = W_0 f(\xi_0) + \sum_{k=1}^{int(n/2)} W_k [f(-\xi_k) + f(\xi_k)] \tag{4.5}$$

where $0 = \xi_0 < \xi_1 < \cdots < \xi_{int(n/2)} \le 1$ and $int(x)$ denotes the integer part of x. The rule is to have precisely n points, so W_0 is zero when n is even.

Being unable to obtain results of the generality of those in §3, we examine specific cases with $p = 1$, 3, and 5. Quadrature rules having the form of (4.5) were either incompatible with (4.4) or produced integration points outside of $[-1,1]$ with even values of p.

4.1. Piecewise-Linear Approximation. With a linear polynomial, the bases for the trial and test spaces are selected as

$$\hat{\mathbf{\Phi}} = \hat{\mathbf{H}} = \{\, \hat{\phi}_{-1}, \hat{\phi}_1 \,\}, \quad \hat{\mathbf{\Psi}} = \{\, \hat{\psi}_{-1}, \hat{\psi}_1 \,\}, \tag{4.6a,b}$$

where $\hat{\phi}_k$, $k = -1$, 1, are given by (2.7b,c) and

$$\hat{\psi}_{\pm 1}(\xi) = \frac{\sinh\sigma(1 \pm \xi)/2}{\sinh\sigma}. \tag{4.6c}$$

Substituting (4.6) into (4.4a) and using (4.5) yields the independent relations

$$X_0 = \frac{4}{\sigma}\tanh(\sigma/2), \quad X_2 = \frac{4}{\sigma}[\coth(\sigma/2) - \frac{4}{\sigma^2}\tanh(\sigma/2)] \tag{4.7}$$

where

$$X_l = \left[\int_{-1}^{1} \xi^l\, d\xi\right]_* = W_0\xi_0^l + \sum_{k=1}^{int(n/2)} W_k[(-\xi_k)^l + (\xi_k)^l]. \tag{4.8}$$

Combined use of (4.8) and (4.7) indicates that there is no quadrature rule with $n = 1$ satisfying (4.7). A two-point quadrature rule exists with $W_0 = 0$ and

$$W_1 = 1, \quad \xi_1 = \sqrt{\coth^2\sigma/2 - 4/\sigma^2}. \tag{4.9}$$

(Scaling of W_1 is arbitrary and we choose unity for convenience.) In the limits as σ tends to zero and infinity, ξ_1 approaches $\sqrt{2/3}$ and 1, respectively. The former case produces an order one quadrature rule and the latter case yields the trapezoidal rule (or the two-point Lobatto formula).

4.2. Piecewise-Cubic Approximation. The bases of the approximation spaces for cubic trial functions are selected as

$$\hat{\mathbf{\Phi}} := \{\hat{\phi}_{-1}, \hat{\phi}_1, \hat{\phi}_2, \hat{\phi}_3\}, \quad \hat{\mathbf{H}} := \{\hat{\phi}_{-1}, \hat{\phi}_1, \hat{\phi}_2, a_3\hat{\phi}_3\}, \quad \hat{\mathbf{\Psi}} := \{\hat{\phi}_{-1}, \hat{\phi}_1, \hat{\psi}_2, \hat{\psi}_3\}, \tag{4.10}$$

where the scaling a_3 is to be determined. Continuity considerations require $\hat{\psi}_i(\pm 1) = 0$, $i = 2, 3$. Additionally, $\hat{\phi}_i(\xi)$, $i \geq 2$, is an odd or even function of ξ when i is, respectively, odd or even (cf. (2.7d)). These restrictions and the use of (4.4a) with $k = 2$, $l = -1, 1, 3$, and $k = 3$, $l = -1, 1, 2$, imply that $\hat{\psi}_2$ is even and $\hat{\psi}_3$ is odd. Thus,

$$\hat{\psi}_2(\xi) = \beta_2[1 - \hat{\psi}_1(\xi) - \hat{\psi}_{-1}(\xi)], \quad \hat{\psi}_3(\xi) = \beta_3[\xi - \hat{\psi}_1(\xi) + \hat{\psi}_{-1}(\xi)]. \tag{4.11}$$

Imposing conditions (4.4a) and solving the resulting system for X_0, X_2, β_2, a_3, X_4, β_3, and X_6 while using (4.11) and

$$-\hat{\psi}''_{\pm 1} + \frac{\sigma^2}{4}\hat{\psi}_{\pm 1} = 0, \tag{4.12}$$

we find

$$X_0 = 2, \quad X_2 = 2/3, \quad \beta_2 = -\frac{1}{\sqrt{6}(1 - \int_{-1}^{1} \hat{\psi}_1(\xi)\, d\xi)}, \quad a_3 = 5(1 - \beta_2 + \frac{8}{\sigma^2}),$$

(4.13a-d)

$$X_4 = m_4 = \frac{2}{3}(2\beta_2 - 1 - \frac{16}{\sigma^2}), \quad \beta_3 = -\frac{1}{\sqrt{10}} \frac{a_3}{1 - 3\int_{-1}^{1} \xi\hat{\psi}_1(\xi)\, d\xi}, \tag{4.13e,f}$$

$$X_6 = m_6 = \frac{2}{3}[-1 + \frac{12}{\sigma^2} + 3(1 - \frac{16}{\sigma^2})m_4 - 4\sqrt{\frac{2}{5}}\beta_3 a_3]. \tag{4.13g}$$

We may use (4.8) to write (4.13a,b,e,g) in the more explicit form

$$W_0 + 2\sum_{k=1}^{int(n/2)} W_k = 2, \quad \sum_{k=1}^{int(n/2)} W_k \xi_k^2 = \frac{1}{3}, \tag{4.14a,b}$$

$$\sum_{k=1}^{int(n/2)} W_k \xi_k^4 = \frac{m_4}{2}, \quad \sum_{k=1}^{int(n/2)} W_k \xi_k^6 = \frac{m_6}{2}. \tag{4.14c,d}$$

A quadrature rule satisfying (4.14) with $n = 4$ and $W_0 = 0$ exists but has ξ_2 outside $[-1,1]$ and, hence, is useless for our application. When $n = 5$, (4.14) describe a one-parameter family of quadrature rules that we specify by selecting $\xi_2 = 1$. In this case,

$$\xi_0 = 0, \quad \xi_1^2 = \frac{m_4 - m_6}{2/3 - m_4}, \quad \xi_2 = 1, \tag{4.15}$$

$$W_0 = 2(1 - W_1 - W_2), \quad W_1 = \frac{1/3 - W_2}{\xi_1^2}, \quad W_2 = \frac{3m_4^2 - 2m_6}{6m_4 - 3m_6 + 2}. \tag{4.16}$$

With all integration points within $[-1,1]$, we find the order-five formula

$$\xi_0 = 0, \quad \xi_1 = \frac{1}{\sqrt{35}}, \quad \xi_2 = 1, \quad W_0 = -8, \quad W_1 = \frac{245}{51,} \quad W_2 = \frac{10}{51} \tag{4.17}$$

as $\sigma \to 0$. As $\sigma \to \infty$, (4.15, 16) give

$$\xi_0 = 0, \quad \xi_1 = \frac{1}{\sqrt{3}}, \quad \xi_2 = 1, \quad W_0 = 0, \quad W_1 = 1, \quad W_2 = 0 \tag{4.18}$$

which is the reduced two-point Gauss-Legendre formula. A seven-point quadrature rule for quintic polynomials is not reproduced here due to its algebraic complexity [21]. It has properties that are similar to (4.15, 16). For example, it approaches a reduced four-point Gauss-Legendre formula as $\sigma \to \infty$.

These surprising results are difficult to understand. Based on the analysis of §3 and §4.1, we would have expected to find formulas that approach Gauss-Legendre quadrature as $\sigma \to 0$ and Lobatto quadrature as $\sigma \to \infty$. Indeed, we shall show in §4.3 that Lobatto quadrature rules produce stable and accurate results for all values of σ. However, unlike the Radau rules discussed in §3, the Lobatto rules apparently do not follow from the

formalism of §4.1 and here.

4.3. Computational Results. Finite element solutions are compared using the special formulas derived in §4.1 or §4.2 and Lobatto quadrature. The Lobatto formulas are chosen to have $p + 1$ points for piecewise polynomial approximations of degree p.

Example 4.1. Consider the two-point problem [16]

$$-\varepsilon^2 u'' + (x^2 + \varepsilon)u = (x^2 + \varepsilon)(1 + \sin\pi x) + \varepsilon^2\pi^2 \sin\pi x, \quad 0 < x < 1, \tag{4.19a}$$

$$u(0) = u(1) = 0, \tag{4.19b,c}$$

which has the exact solution

$$u(x) = 1 + \sin\pi x - u_H(x) \tag{4.19d}$$

where

$$u_H(x) = \frac{1}{\operatorname{erf}(\sqrt{1/\varepsilon})}\{(1 - e^{-1/2\varepsilon})W(x/\sqrt{\varepsilon})e^{-x^2/2\varepsilon} + [1 - e^{-1/2\varepsilon}W(\sqrt{1/\varepsilon})]e^{-(1-x^2)/2\varepsilon}\} \tag{4.19e}$$

and

$$W(z) = e^{z^2}\operatorname{erfc} z. \tag{4.19f}$$

This solution features boundary layers at $x = 0$ and 1. The boundary at $x = 0$ is nearly a second-order turning point.

We solved (4.19) using the finite element method with the special quadrature rules (4.5) on uniform meshes having 10, 20, 40, and 80 elements with piecewise polynomials of uniform degrees $p = 1, 3, 5$. Maximum errors on the 10-element mesh are presented for $\varepsilon = 10^{-3}$, 10^{-5}, and 10^{-7} in Table 2. Similar results appear in Table 3 for computations performed with Lobatto quadrature. A display of $|e^*|_\infty$ as a function of the degrees of freedom and ε is presented in Fig. 7 for the finite element-Lobatto solution. Results with the special quadrature rule (4.5) had a similar behavior. Finally, the exact and finite element-Lobatto solutions with $\varepsilon = 10^{-5}$, $N = 10$, and $p = 1$ to 4 are compared in Fig. 8.

TABLE 2

Maximum errors $|e^*|_\infty$ for Example 4.1 using integration formula (4.5) on uniform N-element meshes with piecewise polynomials of uniform degree p.

p	N	$\varepsilon = 10^{-3}$	10^{-5}	10^{-7}
1	10	0.269(-2)	0.486(-6)	0.487(-10)
	20	0.371(-3)	0.143(-7)	0.143(-11)
	40	0.254(-3)	0.149(-7)	0.150(-11)
	80	0.851(-4)	0.151(-7)	0.151(-11)
3	10	0.437(-2)	0.477(-3)	0.488(-5)
	20	0.382(-4)	0.339(-6)	0.137(-9)
	40	0.272(-6)	0.111(-8)	0.519(-10)
	80	0.127(-7)	0.132(-9)	0.319(-10)
5	10	0.386(-4)	0.905(-3)	0.976(-5)
	20	0.172(-6)	0.926(-6)	0.150(-9)
	40	0.172(-10)	0.401(-12)	0.529(-10)
	80	0.972(-13)	0.597(-12)	0.195(-10)

TABLE 3

Maximum errors $|e^*|_\infty$ for Example 4.1 using Lobatto quadrature on uniform N-element meshes with piecewise polynomials of uniform degree p.

p	N	$\varepsilon = 10^{-3}$	10^{-5}	10^{-7}
1	10	0.777(-2)	0.998(-6)	0.999(-10)
	20	0.201(-2)	0.297(-10)	0.621(-14)
	40	0.546(-3)	0.156(-10)	0.155(-14)
	80	0.140(-3)	0.391(-11)	0.666(-15)
2	10	0.322(-2)	0.998(-6)	0.999(-10)
	20	0.475(-3)	0.947(-10)	0.310(-14)
	40	0.468(-4)	0.782(-11)	0.310(-14)
	80	0.361(-5)	0.195(-11)	0.222(-14)
3	10	0.121(-3)	0.998(-6)	0.100(-9)
	20	0.109(-4)	0.628(-10)	0.488(-14)
	40	0.381(-7)	0.444(-14)	0.621(-14)
	80	0.702(-9)	0.577(-14)	0.288(-14)
4	10	0.118(-3)	0.995(-6)	0.100(-9)
	20	0.636(-6)	0.602(-10)	0.999(-14)
	40	0.769(-8)	0.888(-14)	0.643(-14)
	80	0.328(-10)	0.113(-13)	0.115(-13)
5	10	0.113(-3)	0.985(-6)	0.999(-10)
	20	0.113(-6)	0.528(-10)	0.106(-13)
	40	0.156(-10)	0.999(-14)	0.177(-13)
	80	0.142(-13)	0.126(-13)	0.577(-14)

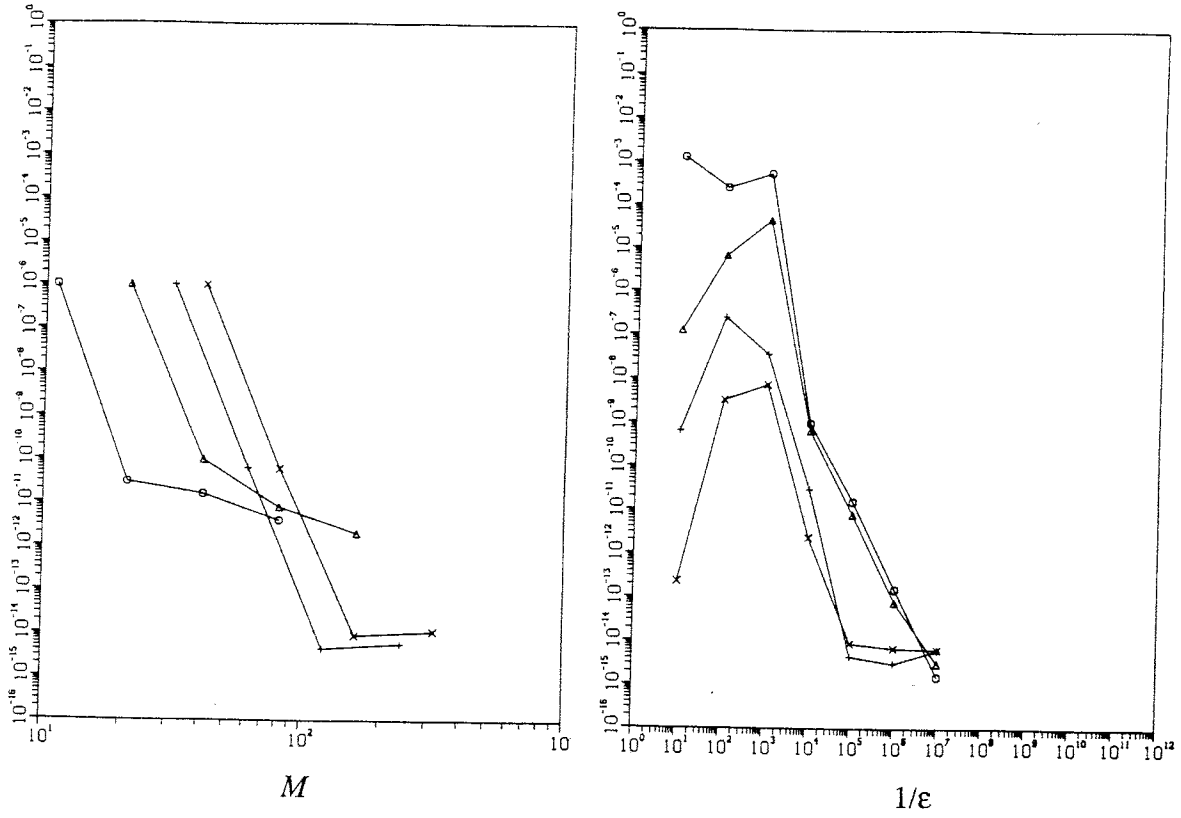

FIG. 7. Maximum errors $|e^*|_\infty$ vs. degrees of freedom M (left) and vs. $1/\varepsilon$ (right) for Example 4.1 using Lobatto quadrature. Uniform mesh and order computations correspond to p = 1 (○), 2 (Δ), 3 (+), 4 (×), and 5 (□).

As with convection-diffusion systems, solutions on Π_{N_1}, presented in Tables 2 and 3 and Fig. 7, have no spurious oscillations for all values of σ. Results using Lobatto quadrature are either comparable or superior to those obtained by the special quadrature rules derived from (4.5); thus, there appears to be little advantage of using the more complex σ-dependent rules. Results presented in Fig. 8 show that boundary layer errors are confined to one element when σ is large. The piecewise-linear solution has no oscillations but higher-order solutions have spurious oscillations within layers that decay in amplitude with increasing p.

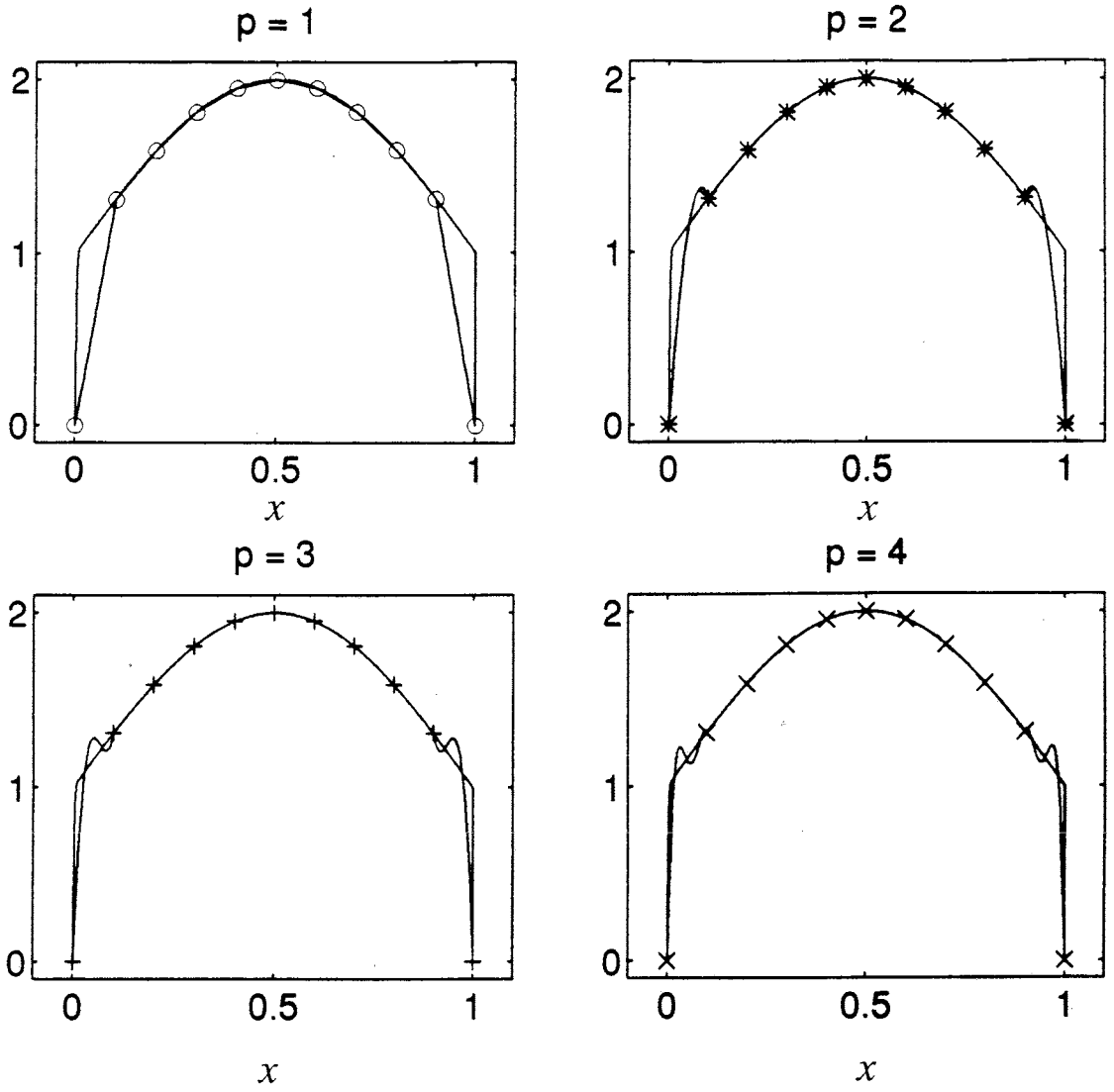

FIG. 8. Finite element solution using Lobatto quadrature and exact solution of Example 4.1 with $\varepsilon = 10^{-5}$, $N = 10$ and $p = 1$ (○), 2 (*), 3 (+) and 4 (×).

5. Two-Dimensional Problems. To have maximal impact, the specialized, Radau, and Lobatto quadrature rules developed and described in §3 and §4 should be applicable to multi-dimensional transient and steady singularly-perturbed partial differential systems. We appraise their suitability in this regard by applying a tensor product of the one-dimensional quadrature rules to three two-dimensional elliptic problems.

Example 5.1. Consider the convection-diffusion equation

$$-\varepsilon\Delta u + 2u_x + u_y = f(x, y), \quad (x, y) \in (-1,1)\times(-1,1), \tag{5.1a}$$

with $f(x,y)$ and the Dirichlet boundary conditions selected so that the exact solution is

$$u(x,y) = (1 - e^{-(1-x)/\varepsilon})(1 - e^{-(1-y)/\varepsilon})\cos\pi(x + y). \tag{5.1b}$$

This solution features $O(\varepsilon)$ boundary layers at $x = 1$ and $y = 1$.

We solved (5.1) with $\varepsilon = 10^{-3}$ and 10^{-6} using the finite element method with a tensor product of the quadrature rules (3.4, 8-10) on uniform square meshes having 8, 16, and 32 square elements per edge and piecewise bi-polynomial approximations of uniform degrees one to four. The maximum pointwise errors measured on the coarse mesh are presented in Fig. 9. Solutions are computed without oscillations for all combinations of ε and N.

Example 5.2. Again consider (5.1a) with $f(x,y) = 0$ and the boundary conditions

$$u(x,0) = 1, \quad u(x,1) = 2, \quad 0 < x < 1, \quad u(0,y) = 2, \quad u(1,y) = 1, \quad 0 < y < 1. \tag{5.2}$$

When ε is small relative to unity, the solution features a sharp wave front that propagates across the domain at an angle of approximately 27° with respect to the positive x-axis.

We solved (5.1a, 2) with $\varepsilon = 10^{-3}$ using the tensor-product quadrature rules (3.4, 8-10) on a 20×20 uniform mesh and piecewise bi-polynomial approximations having degrees one through four. Solutions are displayed in Fig. 10. Like Brooks and Hughes [22], we find solutions with piecewise bilinear approximations to be overly diffusive. Higher-order solutions have less diffusion, but have some spurious oscillations near the wavefront that decrease in amplitude with increasing p. Streamwise upwinding [22] has been used with low-order approximations to remove excessive diffusion near fronts. Perhaps a similar procedure could be developed to further reduce the oscillations associated with higher-order approximations.

Example 5.3. Holland [23] suggested the resonance problem

$$-\varepsilon\Delta u + xu_x + yu_y = 0, \quad -2 < x < 1, \quad -3 < y < 3. \tag{5.3a}$$

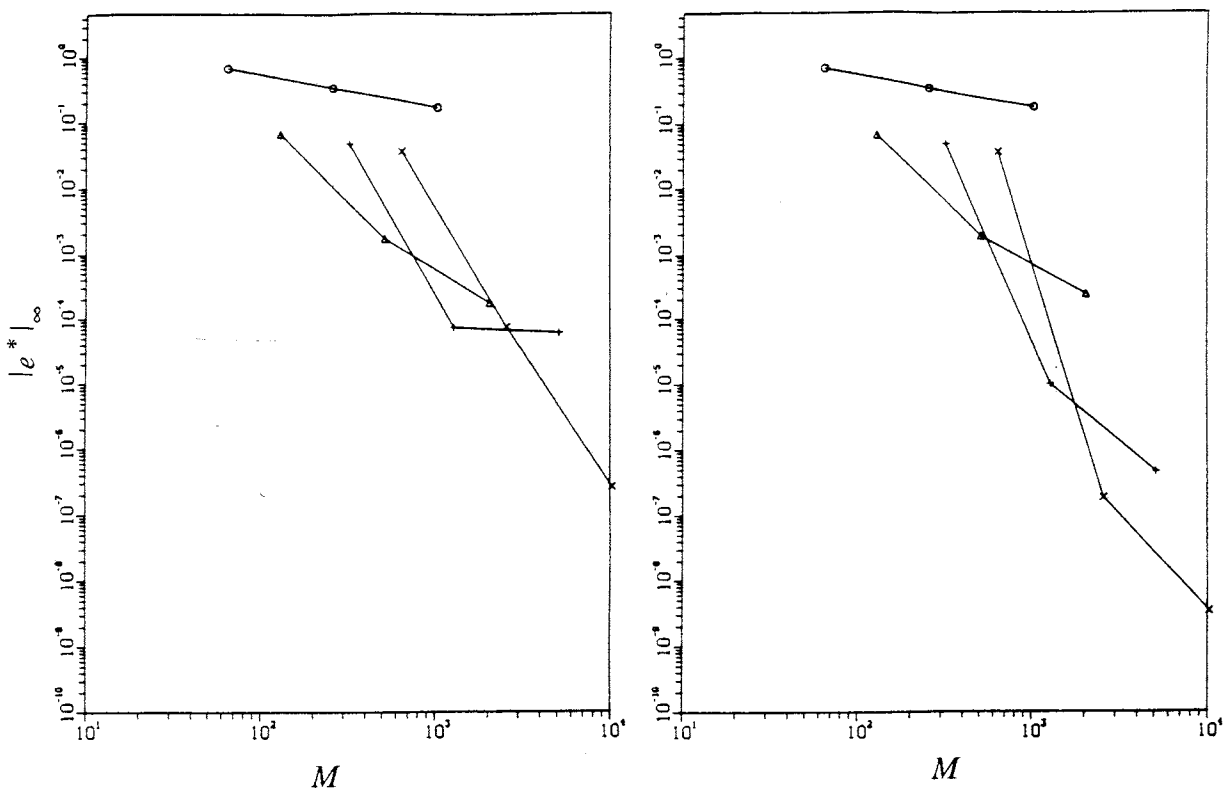

FIG. 9. Maximum errors $|e^*|_\infty$ vs. degrees of freedom M for Example 5.1 with $\varepsilon = 10^{-3}$ (left) and 10^{-6} (right) using a tensor product of the quadrature rules (3.4, 8-10) on uniform square meshes with piecewise polynomials of uniform degree $p = 1$ (O), 2 (Δ), 3 (+), and 4 ($\times$).

$$u(x,-3) = 3, \quad u(x,3) = 5, \quad -2 < x < 1, \tag{5.3b,c}$$

$$u(1,y) = 4, \quad u(-2,y) = 6, \quad -3 < y < 3. \tag{5.3d,e}$$

The usual singular-perturbation theory would indicate that the solution of (5.3) has boundary layers near the edges and is constant in the interior of the domain; however, this theory cannot determine the constant's value. Grassman and Matkowsky [24] used a variational approach to determine the unknown constant as a weighted average of the boundary data at points that are closest to the origin. For the prescribed data and small values of ε, there will be boundary layers except near (1,0), which is the closest point to the ori-

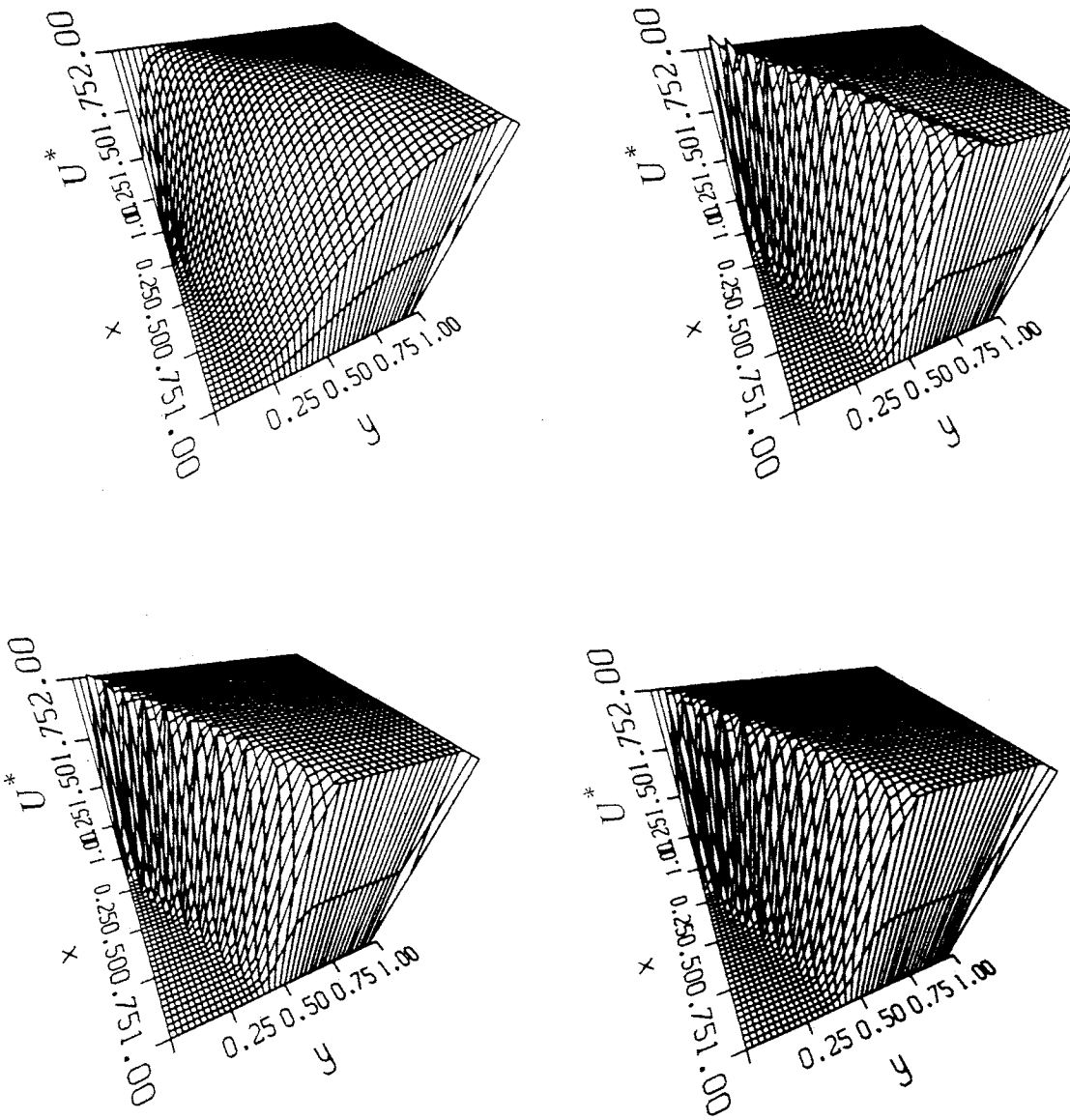

FIG. 10. Solution of Example 5.2 with $\varepsilon = 10^{-3}$ on a 20×20 uniform mesh with piecewise bi-polynomial approximations of degree $p = 1$ (upper left), 2 (upper right), 3 (lower left) and 4 (lower right).

gin. The solution in the interior of the domain will asymptotically be $u(1,0) = 4$.

Holland [23] suggested this problem to test numerical techniques because of its numerous computational difficulties. A transient embedding of (5.3a) in a parabolic problem [2] converges at an exponentially slow rate in ε. When solving the steady problem (5.3), this difficulty gives rise to ill-conditioned discrete systems for large cell-Peclet numbers. Thus, direct solution techniques will be sensitive to round-off error accumulation and iterative solution strategies will quickly converge to a constant interior solution, but take exponentially long to find the correct value.

We solved (5.3) with $\varepsilon = 10^{-3}$, using adaptive h-refinement [2] with piecewise bi-polynomials of degrees one through four. The solution with $p = 1$ is shown in Fig. 11. Solutions did not display any spurious oscillations.

6. Discussion. We have developed a framework for applying the finite element method with high-order approximations to singularly-perturbed differential systems. The method utilizes symbolic techniques to construct quadrature rules for a class of singular-perturbation problems and, herein, we consider convection-diffusion and reaction-diffusion systems. Quadrature rules for convection-diffusion systems tend, as expected, to Gauss-Legendre and Radau integration, respectively, as the cell-Peclet number tends to zero and infinity. Quadrature rules are less understood for reaction-diffusion systems. Formulas for odd-degree polynomial approximations produced stable results but appeared to be sub-optimal. Formulas for even-degree polynomials had evaluation points off the element.

Use of Radau and Lobatto quadrature rules worked extremely well for, respectively, convection- and reaction-diffusion problems. Large errors were confined to elements containing boundary or interior layers for all meshes, orders, and singular-perturbation parameters tested. This is in contrast to the Radau- and Lobatto-based collocation methods of Ascher and Weiss [25] who found oscillations when boundary layers were not adequately resolved. Furthermore, nodal convergence of the Radau- and Lobatto-based finite element

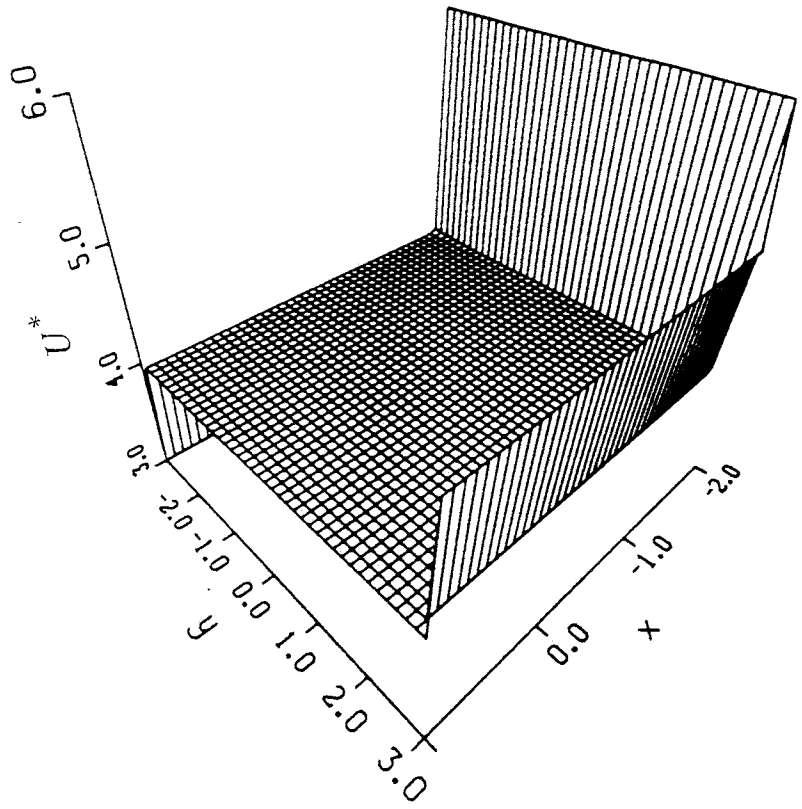

FIG. 11. Solution of Example 5.3 with $\varepsilon = 10^{-3}$ using adaptive h-refinement on an initial 10×10 uniform mesh with piecewise bilinear approximations.

procedures appears to be, respectively, at rates of h^{2p-1} and h^{2p} in the diffusion limit. Thus, nodal superconvergence would seem to be present for both quadrature rules when $p \geq 2$. Global rates of h^p are optimal in energy in the diffusion limit but are, as yet, unknown in the singularly-perturbed limit. Observed accuracy is so high in this case that estimation is not possible. There is little apparent advantage to using the more complex integration procedures of §3 and §4, especially with reaction-diffusion problems. The quadrature framework (§3 and §4) could, of course, be useful with other singularly-perturbed problems. It additionally provides insight as to why Radau quadrature is successful with convection-diffusion problems.

Numerical evidence suggests that the quadrature-based methods work more robustly than anticipated. Thus, for example, methods based on a singular-perturbation analysis of a constant-coefficient two-point boundary value problem provide stable and accurate solutions of two-point problems involving turning points and of partial differential equations. Having stable high-order methods, it becomes possible to use efficient adaptive hp-refinement procedures and we intend to investigate this possibility. Several aspects of the approach are in need of additional analysis before this can be done. A posteriori error estimates, used to guide adaptive enrichment, are needed for each method and quadrature rule. It is likely that such estimates can be developed by p-refinement procedures [10]. Indeed, Biswas et al. [26] used a Radau polynomial to construct error estimation formulas for hyperbolic conservation laws.

A priori error estimates are also needed for the various methods in the different parameter regimes characterized by, e.g., the cell-Peclet number. Streamwise upwinding should also be investigated as a possibility for reducing oscillations near nonuniformities that are oblique to the computational mesh (cf. Example 5.2). Developing such formulas for high-order approximations could be a challenging proposition since streamline curvature may be necessary to maintain high order.

REFERENCES

[1] M. Berger and J. Oliger, *Adaptive mesh refinement for hyperbolic partial differential equations,* J. Comput. Phys., 53 (1984), pp. 484-512.

[2] S. Adjerid, J.E. Flaherty, P.K. Moore, and Y.J. Wang, *High-order adaptive methods for parabolic systems,* Physica D, 60 (1992), pp. 94-111.

[3] K.S. Bey and J.T. Oden, *Analysis of an hp-version of the discontinuous Galerkin method for hyperbolic conservation laws,* 1993, preprint.

[4] J.E. Flaherty and P.K. Moore, *An hp-adaptive method in space and time for para-*

bolic systems, Tech. Rep. 93-15, Dept. Comp. Sci., Rensselaer Polytechnic Institute, 1993.

[5] E. Rank and I. Babuska, *An expert system for the optimal mesh design in the hp-version of the finite element method,* Int. J. Numer. Meth. Engng., 24 (1987), pp. 2087-2106.

[6] J.E. Flaherty, P.J. Paslow, M.S. Shephard, and J.D. Vasilakis, Eds., *Adaptive Methods for Partial Differential Equations,* SIAM, Philadelphia, 1989.

[7] K. Clark, J.E. Flaherty, and M.S. Shephard, Eds., *Adaptive Methods for Partial Differential Equations,* to appear as a special issue of Appl. Numer. Maths., 1994.

[8] K. Eriksson and C. Johnson, *Adaptive streamline diffusion finite element methods for convection-diffusion problems,* Rep. No 1990-18/ISSN 0347-2809, Dept. Maths., Chalmers University of Technology, Goteborg, 1990.

[9] S. Adjerid, J.E. Flaherty, and Y.J. Wang, *A posteriori error estimation with finite element methods of lines for one-dimensional parabolic systems,* Numer. Math., 65 (1993), pp. 1-21.

[10] S. Adjerid, I. Babuska, and J.E. Flaherty, *A posteriori error estimation for the finite element method of lines solution of parabolic systems,* 1993, in preparation.

[11] I. Babuska, T. Strouboulis, and C.S. Upadhyay, *A model study of the quality of a-posteriori estimators for linear elliptic problems. Part Ia: Error estimation in the interior of patchwise uniform grids of triangles,* Tech. Note. BN-1147, Inst. Phys. Sci. Tech., University of Maryland, College Park, 1993.

[12] B. Szabo and I. Babuska, *Introduction to Finite Element Analysis,* John Wiley and Sons, New York, 1989.

[13] P.W. Hemker, *A Numerical Study of Stiff Two-Point Boundary Problems,* Mathemati-

cal Centre Tracts 80, Mathematisch Centrum, Amsterdam, 1977.

[14] U.M. Ascher, R.M.M. Mattheij, and R.D. Russell, *Numerical Solution of Boundary Value Problems for Ordinary Differential Equations,* Prentice Hall, Englewood Cliffs, 1988.

[15] A.M. Il'in, *Differencing scheme for a differential equation with a small parameter affecting the highest derivative,* Math. Notes Acad. Sci. USSR, 6 (1969), pp. 569-602.

[16] J.E. Flaherty and W. Mathon, *Collocation with polynomial and tension splines for singularly perturbed boundary value problems,* SIAM J. Sci. Stat. Comp., 1 (1980), pp. 260-289.

[17] T.J.R. Hughes, *A simple scheme for developing upwind finite elements,* Int. J. Numer. Meth. Engng., 12 (1978), pp. 1359-1365.

[18] K. Sepehrnoori and G.F. Carey, *Numerical integration of semi-discrete evolution systems,* Comp. Meths. Appl. Mech. Engrg., 27 (1981), pp. 45-61.

[19] L.R. Petzold, *A description of DASSL: a differential/algebraic system solver,* Rep. Sand. 82-8637, Sandia National Laboratory, Livermore, 1982.

[20] J. Lorenz, *Nonlinear boundary value problems with turning points and properties of difference schemes,* in W. Eckhaus and E.M. de Jager, Eds. *Theory and Applications of Singular Perturbations,* Lecture Notes in Mathematics, 942, Springer-Verlag, Berlin, pp. 150-169, 1982.

[21] M. Aiffa, *Adaptive hp-Refinement Methods for Singularly-Perturbed Elliptic and Parabolic Systems,* Ph.D. Dissertation, Dept. Math. Sci., Rensselaer Polytechnic Institute, Troy, 1994.

[22] A.N. Brooks and T.J.R. Hughes, *Streamline upwind Petrov-Galerkin formulations for*

convection dominated flows with particular emphasis on the incompressible Navier-Stokes equations, Comp. Meths. Appl. Mech. Engrg., 32 (1982), pp. 199-259.

[23] C.J. Holland, personal communication, 1989.

[24] J. Grassman and B.J. Matkowsky, *A variational approach to singularly perturbed boundary value problems for ordinary and partial differential equations with turning points,* SIAM J. Appl. Math., 32 (1977), pp. 488-596.

[25] U. Ascher and R. Weiss, *Collocation for singular perturbation problems I: First order systems with constant coefficients,* SIAM J. Numer. Anal., 20 (1983), pp. 537-557.

[26] R. Biswas, K. Devine, and J.E. Flaherty, *Parallel adaptive finite element methods for conservation laws,* Appl. Numer. Maths., 1994 to appear.

"High-Order Finite Element Methods for Singularly-Perturbed Elliptic and Parabolic Problems," Workshop on Perturbation Methods in Physical Mathematics, Rensselaer Polytechnic Institute, June 23-26, 1993.

Elaine,

This will appear in the Proceedings of the above. ↑ Joe asked me to forward it for a SCOREC TR.

Thanks

Ron

Call me if I confused you.